Journal of Applied Polymer Science

Microcellular Extrusion of PLA Utilizing Solid-State Nucleation in the Gas-Saturated Pellet Extrusion Process

Dustin Miller, Vipin Kumar
Department of Mechanical Engineering, University of Washington, Seattle, Washington
Correspondence to: D. Miller (E-mail: mille35@uw.edu)

ABSTRACT: In this study, we explore the use of solid-state nucleation in polymer pellets as a means to create microcellular PLA foams in extrusion. This is achieved by using gas-saturated PLA pellets as input to the extruder. Foam density, bubble size, and bubble density is reported and compared with microcellular foams created in the gas-injection extrusion process. PLA pellet gas concentrations between 17 and 29 mg CO_2/g PLA was found to produce quality microcellular foams in this process. Gas concentrations within this range were achieved by varying methods that included partial saturation, desorption from full saturation, and blending saturated with unsaturated pellets. This gas concentration window that produced microcellular foams was found to be independent of the saturation and desorption process used to achieve the desired concentration. We further compare the pressure drop and pressure drop rate of the gas-saturated pellet extrusion process showing that similar foams can be produced at pressures orders of magnitude lower than the alternative gas-injection extrusion processes. Investigations into extrusion pressures support the hypothesis that the gas-saturated pellet extrusion process utilizes solid-state nucleation in the feed section of the extruder to achieve high bubble density foams.

KEYWORDS: foam extrusion; polylactams; microstructure; nucleation

Received 4 November 2011; accepted 24 February 2012; published online
DOI: 10.1002/app.37569

INTRODUCTION

For many years since the invention of solid-state microcellular foams at MIT,[1,2] considerable effort has been spent on developing molten-state extrusion equipment and suitable processing conditions to achieve similar microcellular structures. Cells on the order of 10 μm in diameter define Microcellular foams. There are two important processing requirements for the production of microcellular foams; high nucleation density and controlled cell growth. However, low gas solubility in the melt as well as the fundamental dynamics governing molten-state nucleation poses a challenge to control these morphological characteristics. To overcome these challenges many have had success by increasing the gas delivery pressure; utilizing physical blowing agents such as super-critical CO_2 or N_2 gas injection.[3–13]

Unlike solid-state foam processing where it is relatively simple to create high nucleation densities, molten-state microcellular foam processing using injected gas requires specialized die designs to achieve suitable nucleation densities. These specially designed dies create large pressure drops, which then in combination with high pressure dissolved gas, induce nucleation densities required for microcellular foam growth.[5,6] The challenge of the gas-injection extrusion process lies within the complex design and capital expense of specialized extrusion machinery for both the gas dissolution and bubble nucleation stages. Although, the gas injection extrusion process has found application in industry and a continued research effort by many groups seeks to broaden its uses. Additional research into the addition of nanoparticles to create a large number of heterogeneous nucleation sites within the polymer melt is showing promise, but results remain limited.[14,15]

Microcellular foams research is motivated by the promise for increased mechanical properties over conventional foams such as impact, tensile and fatigue.[16–19] These foams have found a wide variety of applications in packaging, insulation and structural parts. Microcellular Polylactic Acid (PLA) foams have been given great attention in the past few years due to the interest in creating renewable and biodegradable foamed materials. Much academic and industry research is focused on the production of high quality foams that have suitable properties and reduce the overall cost for disposable applications.[20–26] However, PLA presents a significant challenge in creating extruded foams with a narrow processing window.[10,27]

An alternative microcellular extrusion process to the super-critical gas injection method was first proposed and demonstrated in PVC.[28,29] This process differs in the delivery of the blowing agent to the extruder, and the extrusion equipment requirements for nucleation. In this process, pellets are first saturated in a pressure vessel, and then secondarily placed into standard extrusion equipment for foaming. The industrial scale up of this process would require the use of large pressure vessels in order to saturate the polymer pellets with gas. The pressure vessels could either be placed in house, or saturated pellets could be shipped to an extruder after a material supplier saturated them.

In this work we propose new foaming techniques and processing conditions for creating microcellular PLA utilizing the process of saturating polymer pellets with subcritical CO_2 prior to extrusion. Taking advantage of the polymer's high gas solubility at room temperature, saturating PLA pellets in a pressure vessel can accurately control the delivery of blowing agent to the melt without the modification of existing extruder equipment. With a better understanding of the gas diffusion in polymer pellets we then report on the extrusion of PLA foams when varying the amount of blowing agent delivered for foam production.

We further compare the density, average cell size, and bubble density of the foams produced in this study with foams produced by the gas injection extrusion method. Although PLA is typically a challenging material for foam extrusion, the resulting foam morphologies produced from the presaturated pellet extrusion process is shown to create foam morphologies comparable to PLA foams created in the solid-state foaming method.[23] Our results show that pressure drops and pressure drop rates in the gas-saturated pellet extrusion process are order of magnitude lower than those used for gas injection processes, but the bubble densities produced are equivalent. This result shows that solid-state nucleation is preserved in the gas saturated pellet process, decoupling nucleation, and cell growth in the extruder.

EXPERIMENTAL

Materials

All material used in this study was unmodified NatureWorks PLA 4042D. The material was supplied in spherical pellet form with average pellet diameters around 4 mm. Differential scanning calorimetry measurements on the provided material show 4042D PLA has a glass transition temperature 61°C, a peak melting temperature of 151°C, and a pellet crystallinity of 36%. Solid 4042D PLA has a density of 1.24 g/cm^3. Typical applications for this polymer include packaging materials such as films and containers.

Pellet Gas Saturation and Foaming Procedure

The extrusion process includes two distinct stages. A schematic of the full foaming process is shown in Figure 1. The first stage consists of saturating polymer pellets with CO_2 gas in a pressure vessel. Gas saturation took place at room temperature. Saturation and desorption experiments were performed in order to measure the gas diffusion kinetics in PLA pellets. The experimental procedure consists of first measuring the mass of approximately 15 g of PLA pellets; a few hundred pellets in order to average out variations in pellet size. Pellets are then placed in a pressure vessel and pressurized. Periodically the pellets were removed from the pressure vessel and measured on a METTLER AE240 balance with an accuracy of ± 10 μg. Depressurization of the pressure vessel was essentially instantaneous for all measurements and experiments. Gas uptake was measured by the increase in polymer pellet mass. Pellets were then placed back into the pressure vessel to continue absorption. Desorption experiments start by removing pellets from the pressure vessel after saturating, then allowing the pellets to desorb gas at room temperature and pressure. The pellets were periodically weighed to measure the amount of gas that desorbed from the pellets.

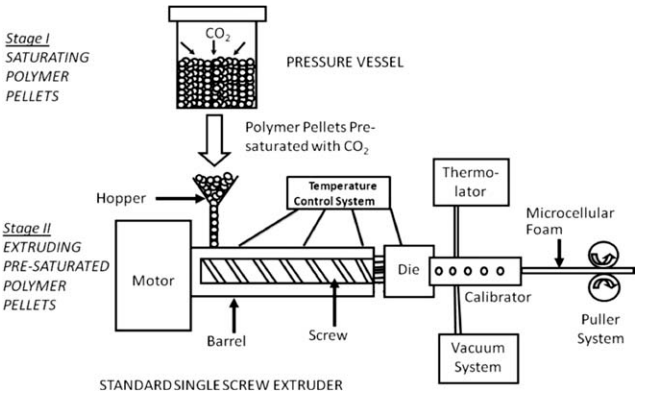

Figure 1. Schematic of the gas-saturated foam extrusion process.

PLA pellets with a diameter of 4 mm absorb CO_2 over many days in the high-pressure environment to bring the material to an equilibrium gas concentration. When pellets are depressurized and placed into the extrusion hopper are still solid and remain unfoamed until they are heated in the extruder. We do not prevent gas from leaving the pellets while in the hopper and thus we must characterize this desorption process. To vary gas concentrations in the polymer during extrusion, pellets were saturated and desorbed of gas by various methods. In some cases the pellets were allowed to reach and equilibrium saturation concentration and allowed to desorb gas over many days. In other extrusion runs pellets were partially saturated and removed from the pressure vessel prior to reaching an equilibrium concentration. Finally, extrusion experiments also blended saturated and unsaturated pellets in a 1 : 1 ratio in order to cut the total amount of gas delivered to the extruder in half.

In the second stage of the extrusion process the unfoamed polymer pellets are placed into the extruder hopper. The standard extrusion setup includes a 3.175 cm diameter single screw extruder with a 22 : 1 *L/D* ratio and a 2.5 compression ratio. A complete convergent die setup (slit size – 3.81 cm × 0.3175 cm) was used to shape the melt. Samples were cut after the die exit and allowed to cool at room temperature in air or an ice water bath to study cooling rate effects. Extrusion temperatures were set and controlled automatically by a temperature control system. Four temperature-controlled locations were measured

and included three along the barrel and one at the die. Extrusion temperature settings ranged between 180/190/196/177°C to 180/190/199/188°C and correspond to the three temperature zones along the screw with the fourth being the die temperature. These temperature settings are slightly reduced from that suggested by the NatureWorks extrusion processing guide which suggests 180/190/200/200°C. Extrusion pressures were measured at the convergent die position and ranged from 1.2 to 2 MPa.

Material Characterization

The density of each sample was determined according to ASTM D792 (densities of plastics using displacement) using a Mettler AE240 analytical scale accurate to 10 μg. Reported density reductions are shown as a relative density compared to the starting solid material. Relative density is defined as the density of the foam divided by the density of the solid. Differential Scanning Calorimetry experiments on the raw material were taken on a TA Instruments Q20. Results for the glass transition temperature, melt peak temperature, and crystallinity are reported in the experimental materials section above.

Samples were imaged with a scanning electron microscope (SEM) to characterize the microstructures produced. All images were taken on a digital FEI Siriron SEM. Polymers samples were first scored with a razor blade and freeze fractured with liquid nitrogen to expose the cross sectional cellular structure perpendicular to extrusion flow. Samples were then mounted in metal stages and the imaged surface was sputter coated with Au/Pd for 50 s. Average cell size was calculated by recording cell diameters of at least 50 cells in the SEM micrograph.

RESULTS AND DISCUSSION

Gas-Saturated Pellet Extrusion

Extrusion runs were conducted at various combinations of saturation and desorption to vary the amount of gas delivered to the extruder. These conditions included partial saturation, long desorption times from full saturation, and blending saturated with unsaturated pellets before placing into the extrusion hopper. The absorption and desorption of CO_2 gas in the spherical PLA pellets was first characterized to show the total gas concentration as a function of time for both the saturation in a pressure vessel and the desorption of gas at ambient conditions. In Figures 2 and 3 we show the gas concentration as a function of saturation and desorption time respectively. The gas saturation processing conditions used in this study and the extrusion results are summarized in Table I, where the gas concentration was determined from the saturation and desorption plots.

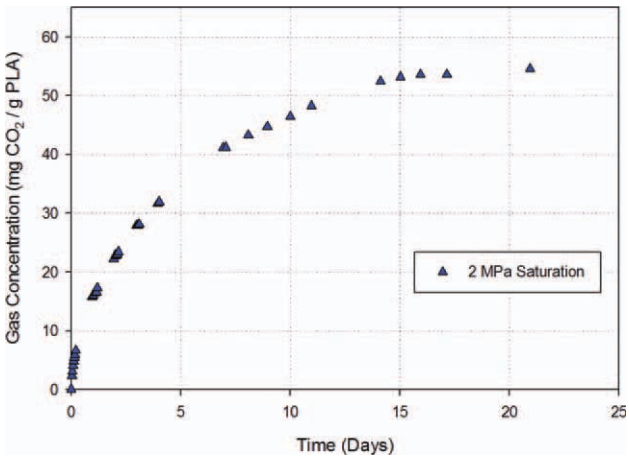

Figure 2. Absorption curve of PLA pellets in CO_2 at 2 MPa. [Color figure can be viewed in the online issue, which is available at wileyonlinelibrary.com.]

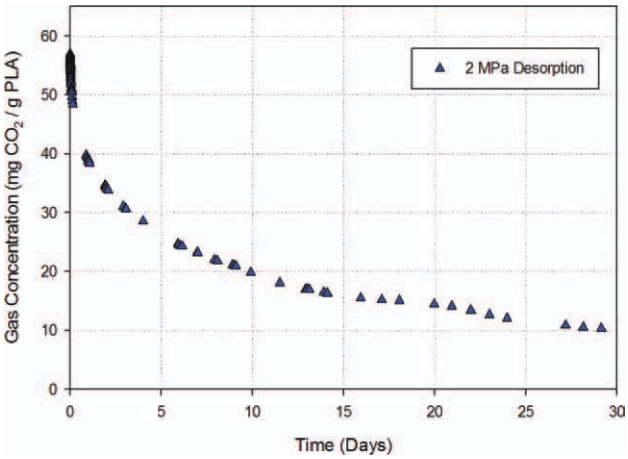

Figure 3. Desorption curve at atmosphere of PLA pellets previously saturated in CO_2 at 2 MPa. [Color figure can be viewed in the online issue, which is available at wileyonlinelibrary.com.]

The saturation conditions used in this study can be broken into three main categories. Experiment numbers 1 to 3 were performed by allowing pellets to absorb gas in a pressure vessel for between 2 and 12 days, times shown in Table I. All of these saturation times are referred to as "partial saturation" because the material was not allowed sufficient time to reach and equilibrium gas concentration. After depressurization the pellets were immediately fed into the extrusion system for processing. A subset of the pellets saturated for 12 days were mixed in a 1 : 1 ratio with unsaturated pellets and extruded. Mixing or blending pellets serves as a novel way to decrease the amount of gas delivered to the extruder. Finally, Experiments 5 through 8 varied the amount of gas delivered to the extruder by controlling desorption of gas after the pellets reached equilibrium in saturation.

In Table I we also summarize the foam densities achieved by the various processing conditions. A significant result from the study found that when pellets were saturated for 12 or 17 days with little or no desorption, the amount of gas dissolved in the pellet was found to be not conducive to foaming. While running these experiments it was observed that at the die exit, large amounts of gas escaped in short bursts and it appeared as though the gas concentration exceeded the solubility limit of the melt at the processing temperature and pressure in the extruder. Others have reported the solubility limit of NatureWorks 3001D PLA at the extrusion temperatures used in this study as being below 20 mg/g.[30]

Table I. Extrusion Processing Conditions

Experiment number	Saturation time (Days)	Desorption time (Days)	Blend ratio (Saturated: Unsaturated)	Gas concentration (mg CO_2 / g PLA)	Densities produced (Relative Density)
1	2	0	1:0	17	66–78%
2	4	0	1:0	28	62–85%
3	12	0	1:0	50	No Foam
4	12	0	1:1	25	72–80%
5	17	0	1:0	56	No Foam
6	17	2	1:0	40	No Foam
7	17	4	1:0	29	62–70%
8	17	6	1:0	24	63–85%

Experiment number 4 sought to reduce the amount of gas being delivered to the extrusion systems by blending 12 day saturated pellets with that of nonsaturated pellets in a 1 : 1 ratio. This effectively reduces the amount of gas concentration by half in the melt. From Table I we can compare the varying amount of gas concentrations. By blending saturated with unsaturated pellets the amount of gas was roughly equivalent to that of a 4-day partial saturation (experiment number 2). The results of blending pellets produced foams equivalent to that of a 4 day saturation in both density and bubble size. Experiments 6–8 were performed by first saturating a large amount of pellets in a pressure vessel for 17 days. After saturation, all pellets were removed from the pressure vessel and allowed to desorb gas at standard temperature and pressure. Batches from this saturation were then processed 2, 4, and 6 days after they were removed from the pressure vessel.

Images taken from the foams produced at all density reducing gas concentrations show that microcellular structures were produced in PLA as long as the gas concentration delivered to the extruder did not exceed 29 mg/g. Microcellular structures are shown in Figure 4 where cell sizes range between 40 and 80 μm in diameter. Cell densities were calculated from the micrographs which were found to range between 2×10^6 to 5×10^6 cells/cm^3. The resulting density data produced from altering the methods of gas delivery to the foam extrusion process show that density is independent of delivery method. Additionally, for gas concentrations between 17 and 29 mg CO_2/g PLA, the microcellular extrusion process can produce stable density results for this system and processing conditions. In Figure 5 we have plotted relative density as a function of die temperature and we can see from this plot that extrusion temperatures can easily control density. This overall discovery allows for much greater flexibility in the processing of microcellular PLA foams by removing the need for specific saturation formulations. As long as gas is delivered within the range, whether by partial saturation, desorption or blending, microcellular structures can be produced.

Kumar et al. proposed that this process allows for solid-state nucleation of the gas-saturated polymer pellets within the compression section of the extruder.[28] It is in this extrusion section pellets reach temperatures close to their glass-transition. Solid-state nucleation in the feed section reduces the need for additional high-pressure nucleation in the die. For this study, extrusion pressure drops in the die of 1.2–2.0 MPa are an order of magnitude lower than that used in gas injection extrusion,[5,6] where pressure drops ranged from 15 to 40 MPa to induce nucleation. The internal extrusion pressures in the gas-saturated pellet process limit the growth of newly formed nuclei. The internal extrusion pressures do not exceed that of the gas saturation pressure and therefore the nucleation sites cannot be dissolved back into the polymer solution.[28] The pressure drop at the die exit, typically a few MPa, then reduces the solubility of the dissolved gas and these large numbers of nucleation sites are free to grow into fully developed bubbles.

Perhaps the most significant finding during the extrusion of the PLA foams was the ability to create quality foam morphologies at low extrusion pressures, on the order of 1.38 MPa. This is significant because alternative microcellular extrusion processes require large pressure drops at the die exit in order to nucleate sufficient bubbles for microcellular expansion. Homogeneous nucleation theory predicts that he cell nucleation rate is given by eqs. (9) and (10), where N_{hom} is the nucleation rate and ΔP is the pressure drop of the gas/polymer solution.[31] Critical importance has been placed on the pressure drop rate of the gas/polymer solution as it moves through the die.[32] Much work has been done on the characterization of bubble density and cell size as a function of pressure drop rate for the gas-injection microcellular extrusion process in order to achieve high bubble densities through the homogeneous, as well as heterogeneous, nucleation.[3,7,9,14,33–35]

$$N_{\text{hom}} = f_o C_o \exp(-\Delta G_{\text{hom}}/kT) \quad (1)$$

$$\Delta G_{\text{hom}} = 16\,\pi\,\sigma_{\text{pb}}{}^3/3\,\Delta P^2 \quad (2)$$

Since the development of the gas-saturated pellet extrusion processes,[28] researchers have proposed that high nucleation densities result from heating gas-saturated pellets in the feed section of the extruder. After solid-state nucleation occurs in the feed section, the internal extrusion pressures subsequently limit cell growth until a point in which the melt is transported to the die exit. Upon exiting the die the pressure drops and allows for cell growth. Support for the solid-state nucleation hypothesis draws on the comparison between the high gas-saturation pressure and the lower extrusion

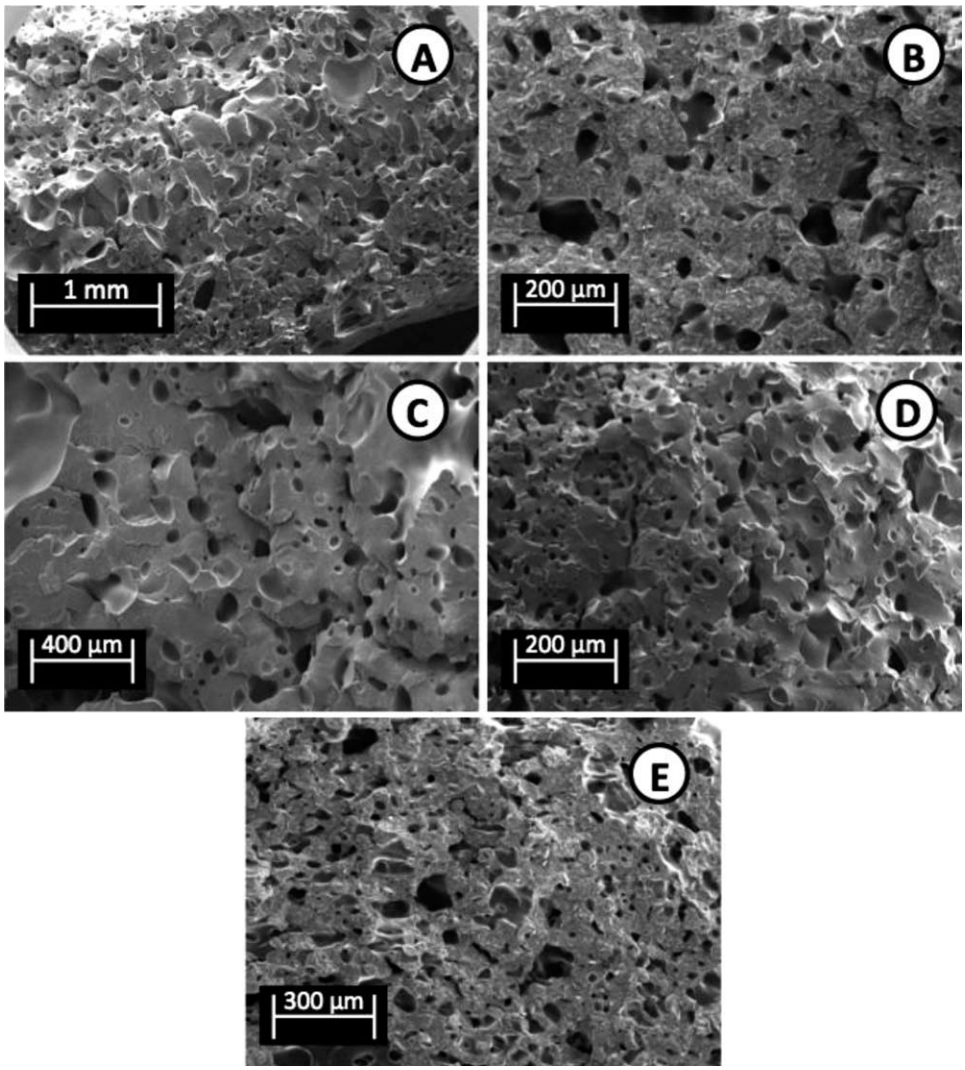

Figure 4. SEM images of microstructures produced. Referencing to Table 1: Sample (A) = Exp. #1, Sample (B) = Exp. #2, Sample (C) = Exp. #4, Sample (D) = Exp. #7, Sample (E) = Exp. #8.

pressures, at least for PVC.[28] It has been shown that after nucleation, newly formed nuclei have an internal pressure equivalent to that of the saturation pressure.[36] The extrusion pressures in the gas-saturated extrusion process are less than that of the saturation pressure and thus limit the dissolution of these newly formed nuclei. Extrusion pressures must exceed that of the nuclei in order to dissolve them back into solution. This hypothesis has historically been difficult to prove since direct observation of the polymer through the extrusion process is not feasible.

It is significant that in this study the extension of an additional polymer system (PLA) also shows that the gas-saturated pellet process, in addition to previous reports on PVC, can produce microcellular structures. After achieving microcellular PLA foams in the gas-saturated pellet extrusion process, it became apparent that a comprehensive comparison between this process and the gas-injection extrusion process could be achieved and that this comparison would further support the concept of solid-state nucleation. We compare the bubble density results achieved for both PVC and PLA in this study to that of the well-established gas-injection foam extrusion process that utilizes pressure drops to control the homogenous nucleation in the polymer melt. In Figures 6 and 7 we show the bubble densities of the foams produced by both process as a function of extrusion pressure and extrusion pressure drop rate at the die.

Comparing the two processes on both extrusion pressure and pressure drop rate we see that the gas-saturated pellet extrusion process achieves, in both PVC and PLA, the highest bubble densities at the lowest processing pressures. The pressure drop rates in the gas-saturated pellet process are roughly 2.5–3 orders of magnitude less than that for the gas-injection processes, yet still produce similar bubble densities. In the case of PVC, the pressure drop rate is 2.5 orders of magnitude less than the closest PS foam, but achieves equivalent bubble densities on the order of 10^8 cells/cm^3. Perhaps one of the greatest differences between the gas-saturated pellet and gas-injected extrusion processes occurs in the PLA foams created in this study. Gas-saturated PLA pellet extrusion produces equivalent bubble densities of 3

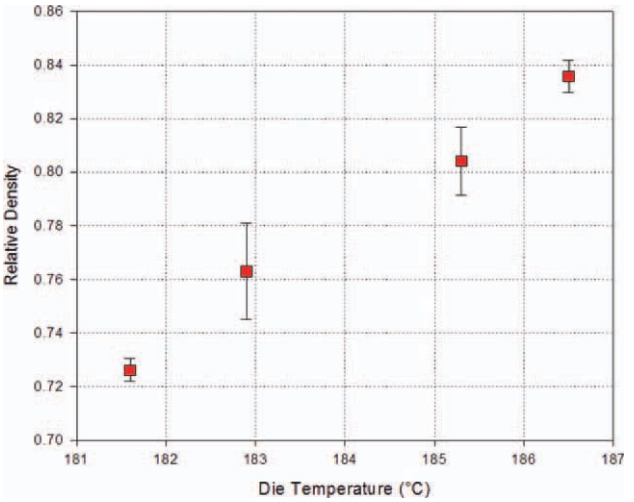

Figure 5. Schematic of the gas-saturated foam extrusion process showing relative density as a function of die temperature. Error bars represent ± 1 standard deviation. [Color figure can be viewed in the online issue, which is available at wileyonlinelibrary.com.]

$\times$ 10^6 cells/cm^3 with extrusion pressures one order of magnitude less than that reported on the PLA gas-injection extrusion process. This is also seen in comparing pressure drop rates where the gas-injection data for PLA foams shows a precipitous drop-off of bubble densities at some of the highest pressure drop rates. No other published work on the gas-injection system has reported bubble densities like that achieved by the gas-saturated pellets extrusion process at similar extrusion pressures or pressure drop rates. It is the characteristics of the gas-saturated pellet extrusion process that allow for these high bubble densities by utilizing solid-state nucleation.

CONCLUSIONS

The gas-saturated pellet extrusion process explored in this work was shown to allow for the microcellular foaming of PLA. Microcellular foamed samples were produced at densities ranging from

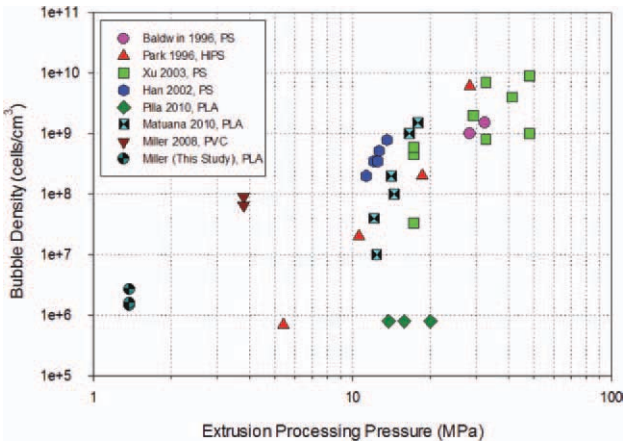

Figure 6. Bubble density as a function of extrusion processing pressure.[3,7,9,33–35,37] [Color figure can be viewed in the online issue, which is available at wileyonlinelibrary.com.]

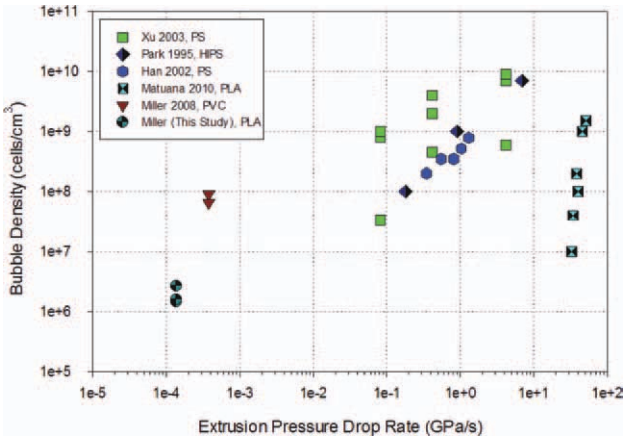

Figure 7. Bubble density as a function of extrusion processing pressure and extrusion pressure drop rate.[3,7,9,33–35,37] [Color figure can be viewed in the online issue, which is available at wileyonlinelibrary.com.]

62 to 85% relative density with cell sizes on the order of 40–80 μm. Partial saturation conditions were used to create these foams where pellets were allowed to saturate for 2–4 days at 2 MPa. These saturation conditions result in gas concentrations of 17 mg/g for 2-day saturation and 28 mg/g for 4-day saturation. Additional foaming experiments were conducted by fully saturating pellets at 2 MPa and allowing to desorb gas for 4–6 days. Densities for this saturation condition ranged from 63 to 85% relative density. Gas concentrations for desorption periods between 4 and 6 days ranged from 24 to 29 mg/g. An alternative method of blending saturated with unsaturated pellets to achieve the desired gas concentration was also found to produce microcellular foams in the extrusion process with gas concentrations of 25 mg/g. This shows that microcellular PLA foams can be achieved in the gas-saturated pellet extrusion process by alternative saturation and desorption methods. The gas concentration range between 17 and 29 mg/g was required to create PLA foams with this process. This result is significant because it shows that the foam created in this study is independent of gas delivery method. The implications to this finding are that the commercialization of this process is more readily achievable before this study. Foam produces using the GSP process can independently coordinate saturation schedules to meet throughput demands rather than worry about how the saturation conditions will influence foam structure.

Prior work done on the GSP extrusion process hypothesized that the process utilized solid-state nucleation as the basis for foam creation. This hypothesis purposes a significant departure from the well-studied microcellular gas-injection extrusion process which uses supercritical gas pressures and a rapid pressure drop device to induce high nucleation densities in the polymer melt. Although logical arguments for the existence of solid-state nucleation in the GSP process have been made, no supporting data had been produced. The question of whether the GSP extrusion process relied on solid-state nucleation became a primary question to investigate in this work, and constituted the most challenging, but most scientifically interesting aspects of this work. The results of this work serve to support the solid-state nucleation hypothesis through indirect evidence of extrusion pressure

drop and pressure drop rates. These pressures are compared with those required for homogeneous nucleation in the gas-injection extrusion process and show that equivalent bubble densities produced by the GSP extrusion process can be achieved at pressure drop rates multiple orders of magnitude lower than the gas-injection methods. The significance of this finding means that the GSP extrusion process can now be shown as a unique microcellular extrusion process to that of other foaming techniques. The GSP extrusion processes ability to separate nucleation from cell growth will serve to motivate future work focusing on exploiting this attribute of the process to potentially achieve greater control and flexibility in foam morphologies.

ACKNOWLEDGMENTS

The research was conducted through the support of grant (#0620835) from the National Science Foundation. Microscopy work was conducted at the Nanotech User Facility at the University of Washington, a member of the National Nanotechnology Infrastructure Network (NNIN) supported by National Science Foundation.

REFERENCES

1. Martini, J.; Waldman, F. A.; Suh, N. P. in SPE ANTEC, San Francisco, CA, **1982,** p 674.
2. Martini, J.; Suh, N. P.; Waldman, F. A. U.S. Pat. 4,473,665 (**1984**).
3. Baldwin, D. F.; Park, C. B.; Suh, N. P. *Polym. Eng. Sci.* **1996,** *36*, 1425.
4. Behravesh, A. H.; Park, C. B.; Venter, R. D. in SPE ANTEC, Atlanta: **1998,** p 1958.
5. Park, C. B.; Behravesh, A. H.; Venter, R. D. *Polym. Eng. Sci.* **1998,** *38*, 1812.
6. Park, C. B.; Suh, N. P. in SPE ANTEC, New Orleans, **1993,** p 1818.
7. Han, X.; Koelling, K. W.; Tomasko, D. L.; Lee, L. J. *Polym. Eng. Sci.* **2002,** *42*, 2094.
8. Shimbo, M.; Nishida, K.; Nishikawa, S.; Sueda, T.; Eriguti, M. *Porous Cell Microcell Mater ASME* **1998,** *82*, 93.
9. Park, C. B.; Suh, N. P. *Polym. Eng. Sci.* **1996,** *36*, 34.
10. Srikanth, P.; Seong, G. K.; George, K. A.; Shaoqin, G.; Chul, B. P. *Polym. Eng. Sci.* **2009,** *49*, 1653.
11. Gendron, R.; Daigneault, L. E. *Polym. Eng. Sci.* **2003,** *43*, 1361.
12. Guo, M. C.; Peng, Y. C. *Polym. Test.* **2003,** *22*, 705.
13. Lee, J. W. S.; Wang, K.; Park, C. B. *Ind Eng Chem Res* **2004,** *44*, 92.
14. Han, X.; Zeng, C.; Lee, L. J.; Koelling, K. W.; Tomasko, D. L. *Polym. Eng. Sci.* **2003,** *43*, 1261.
15. Guo, G.; Wang, K. H.; Park, C. B.; Kim, Y. S.; Li, G. *J. Appl. Polym. Sci.* **2007,** *104*, 1058.
16. Barlow, C.; Kumar, V.; Flinn, B.; Bordia, R. K.; Weller, J. *J. Eng. Mater. Technol.* **2001,** *123*, 229.
17. Collias, D. I.; Baird, D. G.; Borggreve, R. J. M. *Polymer* **1994,** *35*, 3978.
18. Seeler, K. A.; Kumar, V. *J. Eng. Mater. Technol.* **1994,** *116*, 451.
19. Shimbo, M.; Higashitani, I.; Miyano, Y. *J. Cell. Plast.* **2007,** *43*, 157.
20. Kumar, V.; Li, W.; Wang, X. NSF Engineering Research Innovation Conference, Knoxville, Tennessee: **2008.**
21. Lee, S. T.; Kareko, L.; Jun, J. *J. Cell. Plast.* **2008,** *44*, 293.
22. Richards, E.; Rizvi, R.; Chow, A.; Naguib, H. *J. Polym. Environ.* **2008,** *16*, 258.
23. Wang, X.; Kumar, V.; Li, W. *Cell. Polym.* **2007,** *26*, 1.
24. Matuana, L. M. *Bioresour. Technol.* **2007,** *99*, 3643.
25. Matuana, L. M.; Faruk, O.; Diaz, C. A. *Bioresour. Technol.* **2009,** *100*, 5947.
26. Pilla, S.; Kim, S. G.; Auer, G. K.; Gong, S.; Park, C. B. *Mater Sci. Eng.* **2009,** *30*, 255.
27. Kramschuster, A.; Pilla, S.; Gong, S.; Chandra, A.; Turng, L. S. *Int. Polym. Proc.* **2007,** *22*, 436.
28. Kumar, V.; Nadella, K.; Branch, G.; Flinn, B. *Cell. Polym.* **2004,** *23*, 369.
29. Schirmer, H. G.; Kumar, V. *Cell. Polym.* **2003,** *22*, 157.
30. Li, G.; Li, H.; Turng, L. S.; Gong, S.; Zhang, C. *Fluid Phase Equilibra.* **2006,** *246*, 158.
31. Colton, J. S.; Suh, N. P. *Polym. Eng. Sci.* **1987,** *27*, 485.
32. Park, C. B.; Baldwin, D. F.; Suh, N. P. *Polym. Eng. Sci.* **1995,** *35*, 432.
33. Xu, X.; Park, C. B.; Xu, D.; Pop-Iliev, R. *Polym. Eng. Sci.* **2003,** *43*, 1378.
34. Pilla, S.; Kim, S. G.; Auer, G. K.; Gong, S.; Park, C. B. *Mater. Sci. Eng.* **2010,** *30*, 255.
35. Matuana, L. M.; Diaz, C. A. *Ind. Eng. Chem. Res.* **2010,** *49*, 2186.
36. Holl, M. R.; Garbini, J. L.; Murray, W. R.; Kumar, V. *J. Polym. Sci. Part B: Polym. Phys.* **2001,** *39*, 868.
37. Miller, D.; Kumar, V. SPE ANTEC, Milwaukee, WI, **2008.**